Force-induced cell polarisation is linked to RhoA-driven microtubule-independent focal-adhesion sliding

Alexandra M. Goldyn[1,2], Borja Aragüés Rioja[1,2], Joachim P. Spatz[1,2], Christoph Ballestrem[3,*] and Ralf Kemkemer[1,*]

[1]Department of New Materials and Biosystems, Max Planck Institute for Metals Research, 70569 Stuttgart, Germany
[2]Department of Biophysical Chemistry, University of Heidelberg, 69120 Heidelberg, Germany
[3]Wellcome Trust Centre for Cell-Matrix Research, Faculty of Life Sciences, University of Manchester, Manchester M13 9PT, UK
*Authors for correspondence (christoph.ballestrem@manchester.ac.uk; ralf.kemkemer@mf.mpg.de)

Accepted 29 July 2009
Journal of Cell Science 122, 3644-3651 Published by The Company of Biologists 2009
doi:10.1242/jcs.054866

Summary

Mechanical forces play a crucial role in controlling the integrity and functionality of cells and tissues. External forces are sensed by cells and translated into signals that induce various responses. To increase the detailed understanding of these processes, we investigated cell migration and dynamic cellular reorganisation of focal adhesions and cytoskeleton upon application of cyclic stretching forces. Of particular interest was the role of microtubules and GTPase activation in the course of mechanotransduction. We showed that focal adhesions and the actin cytoskeleton undergo dramatic reorganisation perpendicular to the direction of stretching forces even without microtubules. Rather, we found that microtubule orientation is controlled by the actin cytoskeleton. Using biochemical assays and fluorescence resonance energy transfer (FRET) measurements, we revealed that Rac1 and Cdc42 activities did not change upon stretching, whereas overall RhoA activity increased dramatically, but independently of intact microtubules. In conclusion, we demonstrated that key players in force-induced cellular reorganisation are focal-adhesion sliding, RhoA activation and the actomyosin machinery. In contrast to the importance of microtubules in migration, the force-induced cellular reorganisation, including focal-adhesion sliding, is independent of a dynamic microtubule network. Consequently, the elementary molecular mechanism of cellular reorganisation during migration is different to the one in force-induced cell reorganisation.

Supplementary material available online at
http://jcs.biologists.org/cgi/content/full/122/20/3644/DC1

Key words: Force, Mechanotransduction, Focal adhesion, Actin, Microtubules, GTPase

Introduction

Mechanical forces play a crucial role in controlling the integrity and functionality of cells and tissue (Janmey and McCulloch, 2007). External forces are sensed by cells and translated into signals that induce cellular polarisation (Haga et al., 2007; Ingber, 2006; Katsumi et al., 2005). Cyclic stretching of cells is commonly used to mimic external forces exerted in the body (Bao and Suresh, 2003). In such experiments, cells, adherent to an elastic substrate, orient with their long axis perpendicular to the stretch direction (Jungbauer et al., 2008). Such polarisation events require a dramatic reorganisation of the contacts that the cell has with the extracellular matrix (Kaunas et al., 2005; Yoshigi et al., 2005). The direct communication between the cell and the extracellular matrix is mediated by integrins that are associated with the actin cytoskeleton via a multiprotein complex of regulatory molecules (Geiger et al., 2001). Such focal adhesion (FA) sites are thought to be crucial in the process of mechanotransduction and are involved in the transformation of mechanical into biochemical signals (Chen et al., 2004; Geiger et al., 2009).

Force-induced polarisation and reorganisation processes have previously been investigated; however, many details about the molecular mechanisms remain unclear. Little is known about the role of microtubules (MTs) during force-induced cell polarisation, even though they are structurally the stiffest cytoskeletal elements and have demonstrated mechano-responsive functions. MTs grow out to subcellular areas when forces are applied locally (Kaverina et al., 2002; Suter et al., 1998) and their polymeric mass increases rapidly upon single strain steps (Putnam et al., 1998).

MTs are known to regulate FA dynamics during cell migration (Small et al., 2002). Disruption of MTs stops cell migration (Ballestrem et al., 2000; Kaverina et al., 2000), and MT targeting of FAs controls their local stability (Kaverina et al., 1999). Because FAs are crucial for mechanotransduction, a detailed understanding of FA dynamics and regulation is important.

Rho GTPases are key elements in controlling the actomyosin-FA system and MTs play an important role in regulating their activity (Etienne-Manneville and Hall, 2002). Disruption of MTs leads to a stimulation of RhoA activity (Liu et al., 1998), whereas MT re-polymerisation leads to increases of Rac1 activity (Waterman-Storer et al., 1999). Altered activities of RhoA and Rac1 in cyclic stretching experiments have been reported (Kaunas et al., 2005; Liu et al., 2007); however, the results are conflicting. For example, RhoA activity has been reported to both increase (Smith et al., 2003) and remain unchanged (Katsumi et al., 2002; Yamane et al., 2007). Similarly, decreases as well as increases of Rac1 activity have been reported (Katsumi et al., 2002; Yamane et al., 2007). The contribution of MTs in GTPase regulation during the application of stretching forces has not been investigated.

In the present study, we investigated the cellular rearrangements during stretch-induced cell polarisation. In particular, we focused on (1) the role of MTs in FA and cytoskeletal reorganisation, and (2) MT involvement in regulating GTPase activity under mechanical strain. We found that the force-induced cell reorientation is mainly dependent on FA sliding and is largely driven independently of an intact MT network. Although the total RhoA activity increased upon stretch, the total and local Rac1 and Cdc42 activity levels remained unchanged regardless of the presence of intact MTs. Overall, cellular polarisation, including mechanosensing by FAs, the reorientation of the associated actin cytoskeleton, as well as the localised activity of Rho GTPases, seems to be independent of a dynamic MT

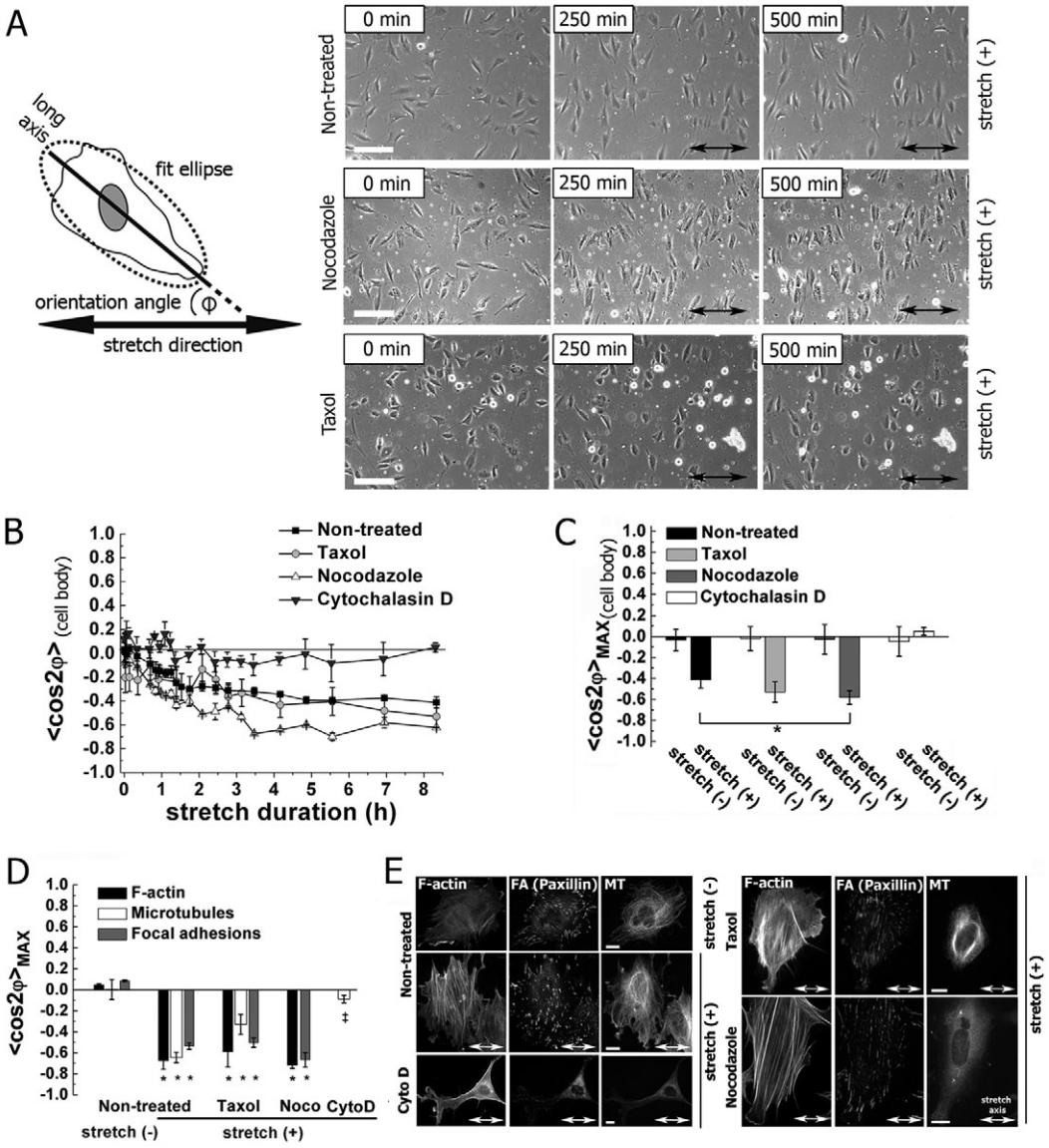

Fig. 1. Stretching forces induces cell repolarisation in a microtubule-independent manner. (A) Cell reorganisation was analysed by fitting an ellipse to each cell outline and measuring the orientation angle, φ, between the long axis of the cell and the stretch direction. Three still images of a time series of an 8-hour phase-contrast movie of stretched (+) non-treated (upper row), nocodazole-treated (middle row) and taxol-treated (lower row) NIH3T3 cells illustrate the cell reorganisation. The direction of cyclic stretch is indicated by the double-headed arrows. Scale bars: 100 µm. (B) Time course of the reorientation of NIH3T3 cells treated with the indicated drugs upon uniaxial cyclic stretching of 8% at 1 Hz. The mean values for the order parameter cos2φ were calculated from the orientation angle φ (see panel A). A value $\langle\cos 2\varphi\rangle = 1$ indicates a perfectly parallel orientation, –1 a perfectly perpendicular orientation and 0 a random cell orientation with respect to the stretch direction. (C) Quantification of the maximum cell reorientation ($\langle\cos 2\varphi\rangle_{MAX}$). The value $\langle\cos 2\varphi\rangle_{MAX}$ resembles the cellular mean orientation of the last 4 hours of cyclic stretch under the indicated conditions. 'Stretch (–)' indicates non-stretched control conditions and 'stretch (+)' the application of cyclic stretch. The disruption of MTs enhanced the cellular reorientation in comparison with non-treated cells (*$P<0.001$). (D) Quantification of F-actin, FA and MT orientation under the indicated conditions after 3 hours of cyclic stretch. Cellular structures were analysed by using fast Fourier transformation (FFT) analysis of cell subareas and background subtraction combined with threshold application to yield $\langle\cos 2\varphi\rangle$ values. The orientation of each analysed structure was significantly higher under non-treated, nocodazole-treated and taxol-treated stretching conditions (+) compared with non-treated, non-stretched conditions (–) (*$P<0.05$). Cells treated with cytochalasin D revealed no difference in alignment of MTs under stretch compared to the non-treated, non-stretched control ($^{\ddagger}P>0.2$). (E) MTs, FAs and actin filaments after 3 hours of cyclic stretch. MTs were visualised by an anti-β-tubulin antibody, FAs were stained with an anti-paxillin antibody and actin was marked using phalloidin. 'Stretch (–)' indicates non-stretched control conditions and 'stretch (+)' the application of cyclic stretch. Actin stress fibres and FAs oriented perpendicular to the stretch direction (double-headed arrow) under non-treated conditions and despite nocodazole or taxol treatment. MT reorientation was dependent on the orientation of the actin cytoskeleton and did not occur in cytochalasin-D-treated cells. Scale bars: 10 µm.

network. This is in contrast to coordinated cell migration, which is strongly dependent on MTs.

Results

Stretching forces induce cell polarisation in a microtubule-independent manner

MTs are thought to be important in the regulation of cell polarisation. To examine the role of MTs as well as actin in the polarisation of cells under mechanical stress, NIH3T3 fibroblasts were exposed to uniaxial cyclic stretching forces (1 Hz, 8% of linear stretch amplitude). For the quantitative analysis of cell polarisation, an ellipse was fitted to the cell outline and the orientation parameter ($\cos 2\varphi$) was calculated as depicted in Fig. 1A, using time-lapse phase-contrast data sets. A time series is given in Fig. 1A as an example illustrating the reorientation for non-treated cells (see also supplementary material Movies 1-4). The maximum mean value of $\cos 2\varphi=1$ indicates a perfectly parallel orientation of the observed cells, and the minimum of –1 indicates a perfectly perpendicular alignment of the cells with respect to the stretch direction (Jungbauer et al., 2008). A mean value of $\cos 2\varphi=0$ corresponds to a random orientation of the cells. Consistent with previous reports (Wang et al., 2007), we found that cyclic stretching leads to the reorientation of fibroblasts perpendicular to the stretch axis. Cells under stretching forces reached a maximum value of $\langle\cos 2\varphi\rangle=-0.4$ after a period of 2 hours (Fig. 1B,C; supplementary material Movie 1). The disruption of the actin cytoskeleton by cytochalasin D completely abolished cellular reorientation (Fig. 1B,C; supplementary material Movie 4). By contrast, neither disruption nor stabilisation of MTs by nocodazole or taxol, respectively, inhibited stretch-induced polarisation (Fig. 1B,C; supplementary material Movies 2 and 3). Disruption of MTs even enhanced the level of cellular reorientation significantly in comparison with non-treated cells ($\langle\cos 2\varphi\rangle_{noco}=-0.6$ versus $\langle\cos 2\varphi\rangle_{non\text{-}treated}=-0.4$; $P<0.001$). Under non-stretched conditions, fibroblasts were randomly oriented (supplementary material Fig. S1).

We next tested whether cellular rearrangements coincided with cytoskeletal and adhesion site reorganisation. Under stretching conditions, both actin filaments and FAs orientated perpendicular to the stretching axis with $\langle\cos 2\varphi\rangle$ of about –0.6. This reorientation was irrespective of MT stabilisation or disruption (Fig. 1D,E). We also analysed how the microtubular network itself is affected by stretching forces and found that MT reorientation reached a similar value of alignment ($\langle\cos 2\varphi\rangle=-0.6$) as the actin cytoskeleton. Although to a lesser degree, MTs stabilised by taxol also realigned perpendicular to the stretching direction. MT reorganisation was, however, completely blocked by the disruption of the actin cytoskeleton with cytochalasin D (Fig. 1D,E), indicating that the microtubular reorientation is tightly linked to the organisation of actin fibres.

Together, these data show that stretching induces cell polarity perpendicular to the direction of stretching. This polarisation depends on an intact actin network but is independent of MT function.

Stretch-induced oriented migration relies on intact microtubules

We next studied cell motility under stretching conditions and tracked cells over a period of 8 hours (supplementary material Fig. S2).

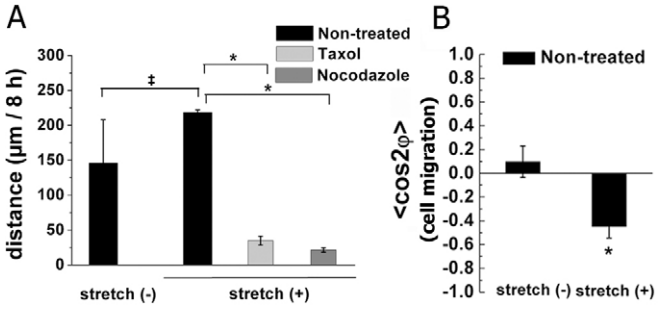

Fig. 2. Stretch-induced, oriented migration relies on intact microtubules. (A) Quantification of NIH3T3 cell-migration distance was performed by tracking the cell nucleus every 10 minutes over 8 hours under indicated conditions. Cyclic stretching at 1 Hz and 8% [stretch (+)] did not significantly change the overall distance of migration compared to non-stretched cells [stretch (–)]. Cell migration was basically blocked by stabilisation (taxol treatment) or disruption (nocodazole treatment) of MTs. ‡No statistical difference, $P>0.05$. *Significance, $P<0.0001$. (B) Oriented fibroblast migration was determined by analysing the linear displacement of non-treated cells from their starting point to their ending point. The direction of migration was perpendicular ($\langle\cos 2\varphi\rangle=-0.45\pm0.1$) during stretching (+) and random ($\langle\cos 2\varphi\rangle=0.1\pm0.13$) under non-stretching conditions (–) (*$P<0.01$).

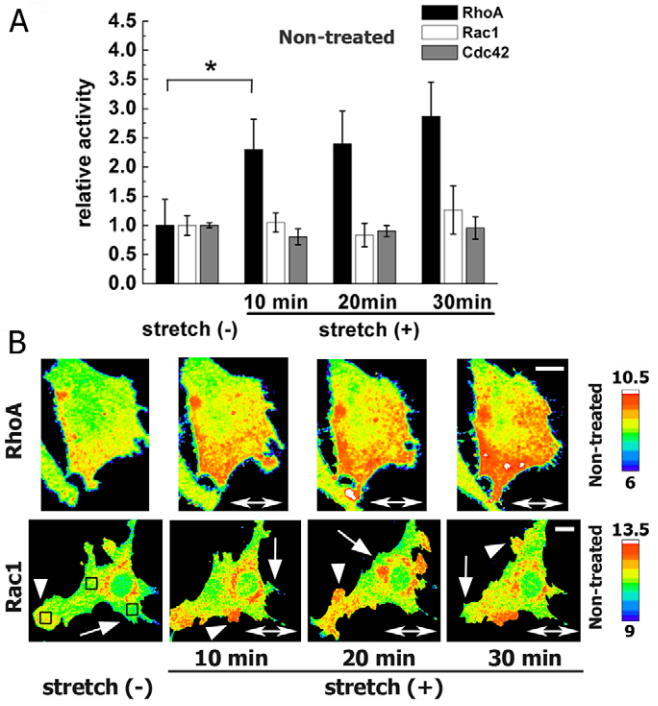

Fig. 3. RhoA activity increases, whereas the activity of Rac1 and Cdc42 remains constant, in response to stretching. (A) For ELISA measurements for active RhoA, Rac1 and Cdc42 proteins, NIH3T3 cells were investigated under non-treated, non-stretched [stretch (–)] and non-treated, cyclic stretched conditions [1 Hz, 8%; stretch (+)] at indicated time intervals. The data set was normalised to stretch (–) measurements. ELISA data show increased RhoA activity levels upon cyclic stretching (*$P<0.01$); Rac1 and Cdc42 activity stays constant. (B) NIH3T3 cells were transfected with either pRaichu-RhoA or pRaichu-Rac1. FRET was determined for non-treated, non-stretched [stretch (–)], and non-treated, cyclic stretched conditions [stretch (+)] at indicated time intervals. FRET images were normalised to the acceptor fluorescence intensity and were displayed using a spectral colour look-up table indicating FRET levels. FRET measurements show that the RhoA activity level increased upon cyclic stretching in a non-polarised fashion (stretch direction is indicated by a doubled-headed arrow). Rac1 activity was high in protruding cell areas (arrowhead) and low in retractions (arrow). Black squares indicate areas of analysis for Rac1 activity gradient (supplementary material Fig. S3). Local Cdc42 activity was high in cell protrusions and did not change upon stretching (data not shown). Scale bars: 10 µm.

Although stretching did not significantly alter the overall distance of cell migration (150 μm over the 8 hours), cells under such forces migrated perpendicularly to the stretch axis (<cos2φ>=–0.45±0.1; P<0.01) as opposed to non-stretched control cells, which migrated in a randomly oriented fashion (<cos2φ>=0.1±0.13) (Fig. 2; supplementary material Fig. S2). Stretch-induced oriented cell migration was essentially blocked by stabilisation or disruption of MTs via treatment with taxol or nocodazole, respectively.

Thus, the presence of dynamic MTs is essential for polarised migration under stretching conditions.

Global RhoA activity increases in response to stretching, whereas that of Rac1 and Cdc42 remains constant

Rho and Rac GTPases have a key role in FA formation, cell polarisation and cell migration (Etienne-Manneville and Hall, 2002). To explore the regulation of GTPases in relation to the observed changes in cell polarity, we tested their activities under stretching conditions. Using the enzyme linked immunosorbent assay (ELISA), we found no changes in Rac1 and Cdc42 activity, but a twofold increase of RhoA activity (P<0.01) after 10-30 minutes of cyclic stretching (Fig. 3A). This increase coincides with normal stress-fibre formation observed in a large variety of cell types (Kaunas et al., 2005; Smith et al., 2003; Yoshigi et al., 2005) (and our unpublished data). We then used fluorescence resonance energy transfer (FRET) reporters to analyse local activity levels of the GTPases. Rac1 activity was usually highest in protruding lamellipodia under both non-stretching and stretching conditions (Fig. 3B; supplementary material Fig. S3), whereas RhoA activity levels rose upon stretching in a non-polarised fashion throughout the cell (Fig. 3B). The highest level of Cdc42 activity was found in the protruding areas of the cells, and levels of local and global Cdc42 activity did not change upon cyclic stretching stimulation (data not shown). We next tested whether inhibition of Rac and Rho activity influenced the polarisation of cells and the cytoskeleton under cyclic stretching. Expression of dominant-negative Rac (RacN17) as well as inhibition of Rho with C3 toxin reduced or inhibited the actin-stress-fibre and cell reorientation, respectively (Fig. 4A,B; compare with Fig. 1D,E). Assessment of MT orientation showed that their reorientation was similar to that of F-actin in RacN17-expressing cells (<cos2φ>=–0.26±0.06). MTs in C3-toxin-treated cells showed a random orientation (Fig. 4A,B). This outlines the dependence of MT orientation on the RhoA-driven orientation of the actin cytoskeleton. In summary, these data show that the stretch-induced polarisation of the actin and MT cytoskeleton is RhoA-dependent, but not Rac1- or Cdc42-dependent.

Microtubules have limited control over (localised) RhoA, Rac1 and Cdc42 GTPase activity

MT disruption is known to increase RhoA activity in adherent and suspended cells (Liu et al., 1998; Ren et al., 1999), an observation that we were able to confirm in our assays. The total RhoA activity increased more than tenfold upon nocodazole treatment in non-stretched adherent cells and 1.2-fold in non-adherent, suspended cells (supplementary material Figs S4 and S5), suggesting that cell adhesion mechanisms are important for reaching maximal RhoA levels. In contrast to RhoA, overall Rac1 and Cdc42 activity levels remained constant after treatment with nocodazole. MT stabilisation by taxol did not show a change of RhoA, Rac1 nor Cdc42 activity levels (supplementary material Fig. S4).

We next explored whether MTs are involved in the regulation of total and localised GTPase activity. FRET and ELISA data

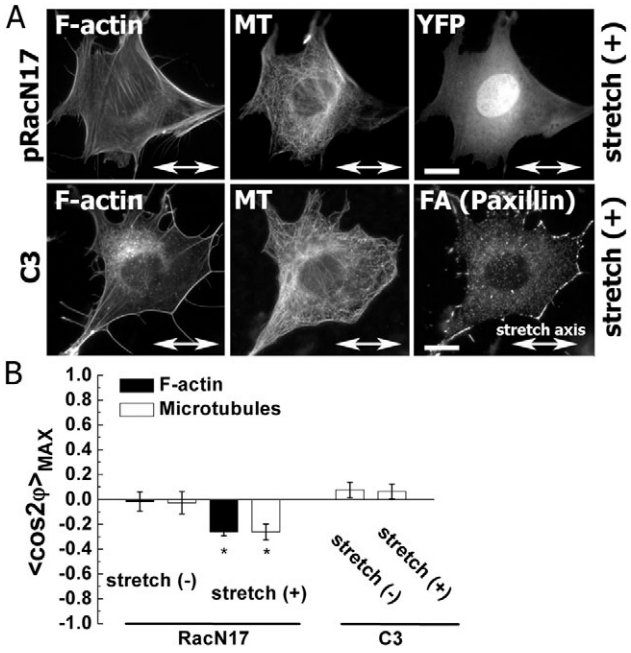

Fig. 4. Inhibition of Rac and Rho activity influences cell and cytoskeleton polarisation under stretching conditions. (A) MTs, F-actin and FAs in NIH3T3 cells subjected to cyclic stretch for 3 hours. MTs were stained by an anti-β-tubulin antibody, FAs were visualised with an anti-paxillin antibody and actin was marked using phalloidin. The direction of cyclic stretch is indicated by a double-headed arrow. Cells either expressed dominant-negative Rac (RacN17) or were treated with C3 transferase for Rho inhibition. RacN17-expressing cells were identified by YFP co-transfection (supplementary material Fig. S6). Scale bars: 10 μm. (B) MT alignment occurred perpendicular to the stretch axis and correlates with F-actin orientation in RacN17-expressing cells (<cos2φ>=–0.26). MTs were randomly oriented in C3-toxin-treated stretched cells (<cos2φ>≈0) (*P>0.05). 'Stretch (–)' indicates non-stretched control conditions and 'stretch (+)' the application of cyclic stretch.

showed no additional increase of RhoA activity under stretching conditions after the disruption of MTs (Fig. 5A,B), which is possibly due to saturated RhoA activity as a result of nocodazole treatment (supplementary material Fig. S4). This finding is supported by our control experiments, because we observed a significant increase in total RhoA activity upon nocodazole treatment also in cells under static, non-stretched conditions (supplementary material Figs S4 and S5). RhoA activity in cells treated with taxol increased similarly to that in non-treated cells upon stretching (Fig. 5A,B; compare Fig. 3A,B). Analysis of Rac1 and Cdc42 activity did not show changes in total or alterations in local activity levels upon treatment with nocodazole or taxol under non-stretching or stretching conditions. The highest Rac1 activity was always found in protruding cell areas and low levels were always in retracting areas of cells (compare Fig. 5A with Fig. 3B; supplementary material Fig. S3). Cdc42 activity levels were similar to those of Rac1, with higher levels in protruding areas and lower activity in the body (data not shown).

To explore whether MT disruption or stabilisation affects protrusion activities, we analysed membrane protrusion formation either perpendicular ('end') or parallel ('side') to the stretch direction (Fig. 5C). Under non-stretched conditions, protrusion activity at cell ends and sides were similar. Cyclic stretching in the horizontal direction doubled the protrusion activity at the ends of the cells, whereas protrusion activity decreased by about half at the

sides of the cell regardless of MT stabilisation or disruption (Fig. 5C).

Together, these data demonstrate that a dynamic MT network is not required to maintain localised activity of tested Rho GTPases and associated protrusive activity of the cells upon induction of directional stretching forces.

Focal-adhesion reorganisation under stretching occurs through sliding mechanisms, which are independent of microtubule dynamics

The data above suggested a dramatic reorganisation of FAs together with the actin cytoskeleton; this reorganisation seemed essentially independent of MTs. Surprisingly, MTs had only limited control over the activity of Rho GTPases, which does not explain why the dramatic reorganisation of FAs is inhibited in cells without MTs during cell migration but not during force-induced polarisation. Therefore, we transfected cells with a GFP-vinculin construct and examined FA dynamics closely by tracking them in time-lapse fluorescence microscopy (Fig. 6; supplementary material Movies 5-10). In contrast to de novo FA formation and disassembly known to be essential for cell migration, stretching forces induced a dramatic sliding of FAs (Fig. 6, left-hand image and enlarged inserts). The observed sliding was not disturbed by disruption nor stabilisation of MTs. Only the orientation of existing FAs but not the number of FAs changed during the period of stretching. Overall, only a very small fraction of FAs was newly formed (<2%); reorganisation occurred rather by growth, shrinking and fusion processes of existing FAs.

These results demonstrate that, in contrast to FAs during cell migration, the FA rearrangements during force-induced polarity are driven by MT-independent mechanisms.

Discussion

This study demonstrates that repolarisation of cells upon cyclic stretching induces sliding of FAs and reorientation of the associated actomyosin machinery. These polarisation events seem to be entirely dependent on downstream RhoA signalling controlling myosin-II function, but they are independent of an intact dynamic MT network.

Because MT depolymerisation induces the formation of actin stress fibres and increases cell contraction via Rho activation (Enomoto, 1996) and MT polymerisation increases Rac1 activity

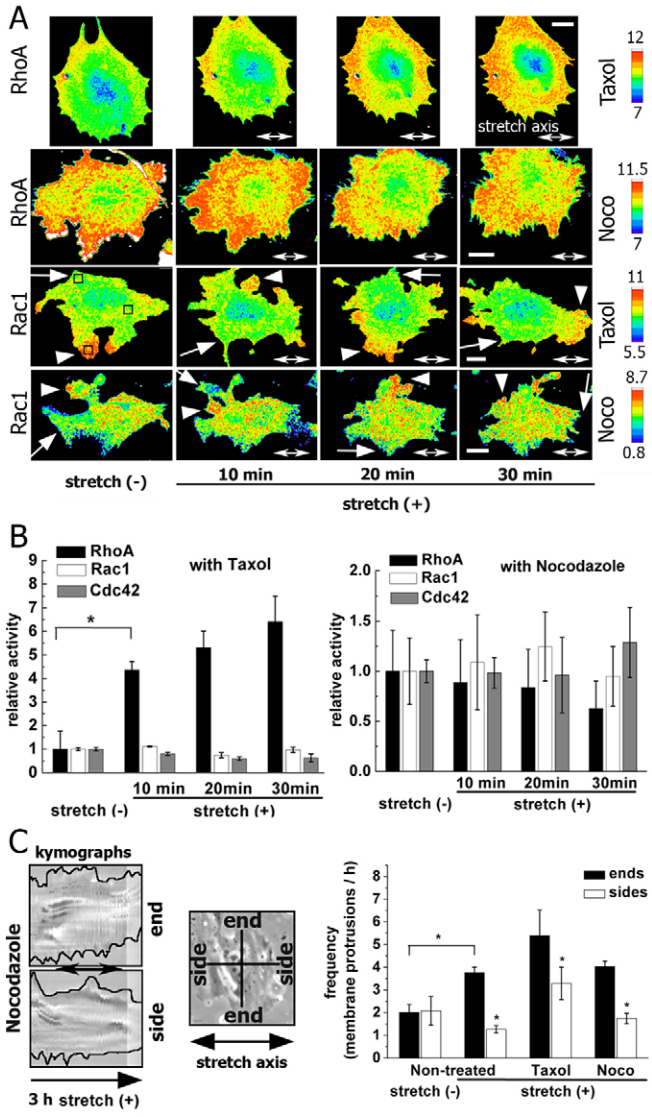

Fig. 5. Microtubules have limited control over (localised) RhoA and Rac1 and Cdc42 GTPase activity. (A) FRET measurements for RhoA and Rac1. NIH3T3 cells were transfected with either pRaichu-RhoA or pRaichu-Rac1 and treated with taxol or nocodazole prior to the FRET measurements. FRET was determined for non-stretched [stretch (–)] and cyclic stretching [1 Hz, 8%; stretch (+)] conditions at indicated time intervals. FRET images were normalised to the acceptor fluorescence intensity and are displayed using a spectral colour look-up table indicating FRET levels. RhoA activity increased upon cyclic stretching independent of MT stabilisation with taxol (stretch direction is indicated by a double-headed arrow). RhoA activity was high upon disruption of MTs (nocodazole) and did not further increase upon stretching. Under all conditions (taxol or nocodazole treatment), Rac1 activity levels were high in protruding cell areas (arrowhead) and low in retractions (arrow). Black squares indicate areas of analysis for Rac1 activity gradient (supplementary material Fig. S3). Local Cdc42 activity did not change upon application of cyclic stretch (data not shown; refer to the Results section). Scale bars: 10 μm. (B) For ELISA measurements for active RhoA, Rac1 and Cdc42 proteins, NIH3T3 cells were treated with either taxol or nocodazole and investigated under non-stretched [stretch (–)] and cyclic stretching conditions [stretch (+)] at the indicated time intervals. The data set was normalised to stretch (–). ELISA data show an increase in RhoA activity upon stretch in presence of taxol (**P*<0.01). Cyclic stretching did not further increase RhoA activity in nocodazole-treated cells (compare with A). Rac1 and Cdc42 activity in taxol- and nocodazole-treated cells did not change upon stretching. (C) Kymograph analysis of directional NIH3T3 protrusion activity over a time course of 3 hours. The direction of stretch is indicated by a double-headed arrow. To illustrate the analysis, a nocodazole-treated cell is displayed. A line was drawn along the cell edge of a composite phase-contrast image and the peaks were counted to yield a frequency of membrane protrusions per hour. Cell protrusions occurring perpendicular to the stretch axis were determined as ‘end’; cell protrusions parallel to the stretch direction were called ‘side’. Application of stretching doubled the protrusion activity at the ends but decreased activity by about half at the sides of cells (**P*<0.01). Independent of MT stabilisation (taxol) or disruption (nocodazole), the rate of protrusions remained higher at ends compared with those measured at the sides of the cells (**P*<0.01).

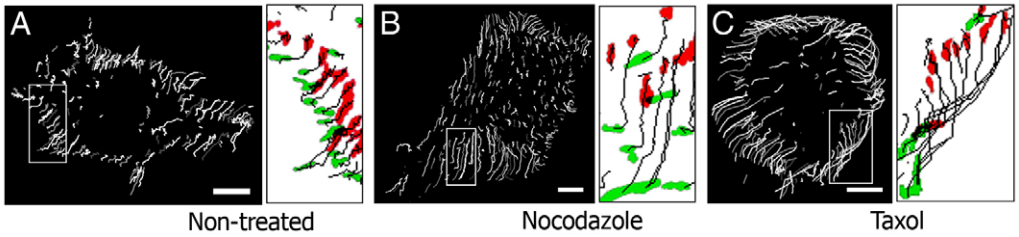

Fig. 6. FA reorganisation occurs through a MT-independent sliding mechanism. FA dynamics was investigated in cells subjected to cyclic stretch of 8% at 1 Hz under indicated conditions (a, non-treated; b, nocodazole-treated; c, taxol-treated). NIH3T3 cells were transfected with pGFP-vinculin and time-lapse fluorescent movies were recorded (see supplementary material Movies 5-10). Grey-scale images on the left of each condition show single FA tracks over a time period of 115 minutes for non-treated and 180 minutes for nocodazole- and taxol-treated cells. Enlarged areas are indicated by white boxes. Selected FAs are colour-coded: green for FAs before stretch application (0 minutes), red for FAs after stretch (for non-treated after 100 minutes, for nocodazole and taxol after 160 minutes). Scale bars: 10 μm.

(Waterman-Storer et al., 1999), we assumed that MTs would play a crucial role during polarisation of cells stimulated by mechanical forces. However, we found very little impact of MTs with respect to two main aspects directing cell polarity: (1) the actin cytoskeleton and FA rearrangements seemed similar at stretching conditions, and (2) there was surprisingly little effect on total and local activity levels of Rac1 and Cdc42 in cells, neither under stretching conditions nor in the presence of reagents stabilising or disrupting MTs. However, a certain level of RhoA activity is essential for the polarised reorientation of cells, because blocking RhoA activity with C3 transferase inhibited polarisation in our experiments. A moderate increase in RhoA activity might result in an enhanced reorganisation of actin stress fibres (Kaunas et al., 2005). By contrast, non-physiological expression of constitutively active RhoA (RhoV14) blocked the rearrangement of actin fibres (our unpublished observation). This suggests that RhoA-activity modulation is important for polarised rearrangements and disturbance leads to impaired actin reorientation.

The slight but significantly increased level of reorientation in cells treated with nocodazole compared to non-treated cells suggests that MTs contribute to some extent to the observed polarisation events by influencing RhoA activity. One way by which MTs could contribute to the faster polarisation events might be regulation of GEF-H1, because release of GEF-H1 from MTs has been shown to enhance RhoA activity and actin stress-fibre formation (Krendel et al., 2002). GEF-H1 activation, however, is less likely to contribute to the force-induced RhoA activation per se, because RhoA activity still increases upon force application when MT dynamics are inhibited by taxol. Other guanine-nucleotide exchange factors (GEFs), such as p190RhoGEF and PDZ RhoGEF, that localise to FAs and are involved in regulating RhoA activity (Iwanicki et al., 2008; Lim et al., 2008; Tomar and Schlaepfer, 2009) might be potential candidates with respect to the reorganisation of FAs and the upregulation of RhoA activity upon stretching forces.

We assume that the stretch-induced increased RhoA activity stems from force transduction in FAs. A positive biomechanical feedback loop has been suggested in which increased tension in actin stress fibres, either by the internal actomyosin system or external stretch, activates RhoA at FA sites and increases, in turn, stress-fibre assembly (Besser and Schwarz, 2007). In fact, FAs and the molecules therein are one of the primary receptors for mechanical cues, which are then transmitted to the actin cytoskeleton (Geiger and Bershadsky, 2002). One of the candidates might be vinculin, which has been recently shown to provide a major link of the FA plaque to the actin cytoskeleton (Humphries et al., 2007).

MTs target FA (Krylyshkina et al., 2003) and are vital for FA turnover during cell migration (Kaverina et al., 2000). The observed massive FA reorganisation during stretch-induced cell repolarisation was not affected by the absence of MTs. We showed that essentially all FA rearrangements, after application of directional cyclic stretching, are accomplished by sliding and not by de novo formation. These sliding FA rearrangements were irrespective of the presence or absence of MTs. Therefore, it seems probable that reorganisation of cell-matrix adhesions during migration is controlled by molecular mechanisms that are different from those for cell polarisation under cyclic stretching. The precise molecular cues that are involved in FA sliding remain to be investigated. However, one reason for the difference between stretch-induced FA sliding and coordinated cell migration might be that the latter depends on MT-guided shuttling of large numbers of vesicles that fuse with the outer membrane for protrusive activities (Schmoranzer et al., 2003). Disruption or stabilisation of MTs would then compromise vesicular transport to some extent, leading to the inhibition of cell migration (Schmoranzer et al., 2003).

The cellular tensegrity model suggests that MTs build a rigid frame that resists actomyosin contraction (Ingber, 2006; Stamenovic et al., 2002), but it is also well known that MTs are highly dynamic (Wehrle-Haller and Imhof, 2003). We showed that MTs are obviously guided by actin filaments and consequently follow actin-stress-fibre orientation, as is also observed in neuronal cells, in which actin bundles provide guiding cues for MTs (Zhou et al., 2002). It is likely that molecules such as ACF7, which has been shown to regulate guidance of MTs along filamentous actin (Kodama et al., 2003), could facilitate the microtubular reorientation.

We observed that the overall cell displacement per time unit did not vary between non-treated non-stretched and non-treated stretched conditions. If stretched, the cells migrated preferentially perpendicular to the stretching direction, which resembles a one dimensional (1D)-like random walk. By contrast, a random migration in 2D is observed if no stretch is applied. In theory, one would expect a twofold higher displacement of cells on static substrates (2D migration) compared with cells on stretched substrates (1D-like migration) considering that the mean square displacement (MSD) is given by $MSD=2\times d\times D\times t$ (with D the diffusion constant, t the time and d the dimension of walk). We attribute the deviation of our results from the expectation that the displacement rate should be increased on stretch to the observed higher protrusion activity perpendicular to the stretch direction, which might lead to a higher effective diffusion constant for cells on stretched substrates, thus resolving the apparent discrepancy.

In conclusion, we have demonstrated that RhoA-driven actomyosin machinery controls polarised rearrangements of the cell, their cytoskeleton and FAs. In striking contrast to the important role of MTs for FA assembly and disassembly during cell migration, MTs are not required for FA sliding during cell polarisation under mechanical stretching forces. We conclude that cell migration and force-induced cell polarisation are directed by different molecular cues.

Materials and Methods

Cells and plasmids

NIH3T3 (from DSMZ, Braunschweig, Germany) were cultured in DMEM (Invitrogen, Karlsruhe, Germany) supplemented with 10% FCS (Invitrogen). pEYFP-N1 and pECFP-N1 were from Clontech Laboratories (Saint-Germain-en-Laye, France); the FRET probes pRaichu-Rac, pRaichu-RhoA and pRaichu-Cdc42 were a kind gift from Michiyuki Matsuda (Itoh et al., 2002).

Cell-stretching experiments and light and fluorescent microscopy

Stretching experiments were performed as described in great detail elsewhere (Jungbauer et al., 2008). Briefly, 50 cells/mm^2 were plated on fibronectin (20 μg/ml) (Sigma-Aldrich, Munich, Germany)-coated poly(dimethylsiloxane) (PDMS; Corning Sylgard, Midland, MI) elastomeric membranes. The stretching device was mounted on an inverted light microscope (AxioVert 200M, 10×/0.25Ph1 objective, Zeiss, Jena, Germany) equipped with a CCD camera (PCO Sensicam, Kelheim, Germany) or an upright light microscope (AxioImager Z1, W-Plan Apochromat 63×/1.0 VIS-IR water-immersion objective, Zeiss) with an AxioCam CCD camera. A self-developed software routine embedded in Image Pro 6.2 (Media Cybernetics, Bethesda, MD) or AxioVision 4.6.3.0 (Zeiss) was used. Images for time-lapse phase-contrast movies were acquired at 50-second or 100-second intervals for the indicated time periods using DMEM supplemented with 10% FCS (Invitrogen) and 1% penicillin-streptomycin (Gibco). Images for time-lapse fluorescent movies were taken every 5 minutes or 10 minutes for the indicated time periods using carbonate-free Ham's F-12 media with L-glutamine (Sigma) with 2% FCS (Invitrogen), 25 mM HEPES (Sigma) and penicillin-streptomycin (Gibco). Parameters for cyclic stretching were set to 1 Hz and 8% of linear stretch amplitude. For each experimental condition at least three movies were acquired.

Chemical inhibitors and transfections

Concentrations of 3 μM taxol, 3 μM nocodazole and 1 μM cytochalasin D (all Sigma) were used and cells pre-incubated for about 30 minutes. C3 transferase (Cytoskeleton, Denver, CO) was used according to the manufacturer's manual. Transient transfections were performed with Lipofectamine 2000 (Invitrogen) as recommended by the manufacturer.

Cell staining

Cell staining was performed as described previously (Humphries et al., 2007). Rabbit monoclonal (Y113) anti-paxillin antibody and anti-Myc clone 9E10 antibody were from Abcam (Cambridge, UK); the mouse monoclonal anti-β-tubulin (clone TUB2.1) was from Sigma. The secondary antibodies (goat anti-mouse Alexa Fluor 350 and goat anti-rabbit Alexa Fluor 568) and Alexa-Fluor-488 phalloidin were all from Invitrogen.

Myc-tagged pRacN17 and pEYFP-N1 vectors were expressed in a 2:1 ratio and showed coexpression efficiencies of about 95% (supplementary material Fig. S6).

The fluorescent images of fixed cells were contrast enhanced.

Analysis of the orientation of the cell, actin stress fibres, microtubules and focal adhesions

Cell orientation (Fig. 1A) was measured as described previously (Jungbauer et al., 2008). Briefly, phase-contrast images in order of their acquisition were taken and the cell outline of each single cell was marked. An ellipse was fitted to each cell outline. The orientation angle, φ, of the long axis of the ellipse with respect to the stretch direction was measured (Fig. 1A). The mean values for the order parameter cos2φ were calculated from the orientation angle φ and $\langle\cos 2\varphi\rangle$ denotes the mean value of the orientation parameter. A value of $\langle\cos 2\varphi\rangle=0$ corresponds to cells that were randomly oriented, $\langle\cos 2\varphi\rangle=1$ if all cells were parallel oriented, and $\langle\cos 2\varphi\rangle=-1$ if they were perpendicularly oriented with respect to the stretch axis. The time series of nocodazole-treated stretched NIH3T3 cells in Fig. 1A were contrast enhanced. The value for the maximum cell reorientation $\langle\cos 2\varphi\rangle_{MAX}$ resembles the mean orientation value of the last 4 hours of cyclic stretch under the indicated condition.

For analysis of actin-stress-fibre and MT orientation (Fig. 1D; supplementary material Fig. S7A) a self-developed software macro embedded in ImageJ (http://rsb.info.nih.gov/ij/) was used. Subareas of a cell were analysed by texture analysis via a fast Fourier transformation (FFT) in analogy to Kemkemer et al. (Kemkemer et al., 2000). In brief, each cell picture was divided into many small squares (64×64 pixels). For each square, a FFT was performed and the resulting image was further analysed to measure the mean orientation of fibres within the square. The measured angles of orientation of actin stress fibres or MTs within the analysed square were plotted into the image, where the *x*-axis of the image indicates the direction of stretch or an arbitrary *x*-axis in the non-stretched case (supplementary material Fig. S7A). The mean value ($\langle\cos 2\varphi\rangle$) of all analysed cell subareas was calculated and yielded in a mean orientation value for actin stress fibres or MTs of a single cell. The angle for FA orientation (Fig. 1D; supplementary material Fig. S7B) was measured with ImageJ and expressed as a $\langle\cos 2\varphi\rangle$ value. Briefly, FAs were separated from the background by using the threshold tool of ImageJ and a mask of FAs was generated (supplementary material Fig. S7B). The orientation of the mostly elliptic FAs was determined using the measurement tool in ImageJ. The obtained angles were then transformed into the mean value ($\langle\cos 2\varphi\rangle$) for each single cell. In total, 20-30 cells from three independent experiments were evaluated for actin (stress) fibre, MT and FA orientation.

FA sliding was analysed using Manual Tracking in ImageJ. A minimum of three cells was analysed for each condition.

Analysis of migration and cell protrusive activity

Migration was measured by tracking the cell nucleus using ImageJ. For each experimental condition, a minimum of ten cells was analysed. Images were captured every 10 minutes over 8 hours from at least three independent experiments. The orientation during cell migration was determined by analysing the linear displacement of a cell from its starting point to its ending point; the obtained angle (φ) of the straight line with respect to the stretch axis was transformed into cos2φ values (Fig. 2B).

Membrane protrusive activity was quantified by kymograph analysis of ImageJ as described previously (Ballestrem et al., 2000; Humphries et al., 2007). Briefly, the single images were lined up on a time scale in order of their acquisition. The resulting composite phase-contrast picture allowed us to continuously follow the translocation of recorded structures over time. Membrane protrusions were identified by their characteristic centripetal movement, beginning at the lamella edge. A line was drawn along the cell edge and the peaks were counted to yield a frequency of membrane protrusion per hour. Dynamics of ten cells from at least three independent experiments were studied at intervals of 50 seconds over the time course of 3 hours (Fig. 5C).

FRET analysis

FRET reporters were transfected and cells were plated on the elastic membranes as explained above. The filter sets used were: for CFP: 54HE; YFP: 46; FRET: BP 535/30, DBP 464/32, and 547/43, excitation 54HE (all from Zeiss). Cells were illuminated with a lambda-DG4 Xenon lamp (Sutter Instrument Company, Novato, CA) and imaged in carbonate-free Ham's F-12 media with L-glutamine (Sigma) with 2% FCS (Invitrogen), 25 mM HEPES (Sigma) and penicillin-streptomycin (Gibco). Following stretching, a set of three images – (1) excitation (Ex) CFP/emission (Em) CFP; (2) ExCFP/Em YFP (FRET filter); (3) ExYFP/Em YFP – was captured at the indicated time intervals. The function of the FRET constructs was tested to report GTPase activity by addition of serum to starved cells. The calibration experiments showed a similar outcome as originally published (Itoh et al., 2002; Zaidel-Bar et al., 2005).

For image analysis, the PixFRET plug-in (Feige et al., 2005) for ImageJ was used. Calculation of FRET images was done as described in detail previously (Ballestrem et al., 2006). Briefly, FRET was calculated from all recorded channels for pixels above background levels. The FRET values were corrected for the bleed-through of the CFP and YFP channel and normalised to the acceptor fluorescence intensity; bleaching of CFP and YFP was negligible under the settings we chose for the experiments. FRET images were displayed using a spectral colour look-up table indicating FRET levels.

Rac1-, Cdc42- and RhoA-activity assay

The Rac1-, Cdc42- or RhoA-activity assay was performed with a commercially available ELISA Kit (Cytoskeleton) and experiments were performed as described in the manufacturer's manual. Luminescence (RhoA, Rac1) readout or absorbance$_{(OD490\ nm)}$ (Cdc42) for evaluation of Rho GTPase activities was detected with a fluorescence spectrophotometer (Tecan, Crailsheim, Germany). The obtained values were normalised to one for the non-treated non-stretched condition.

Statistical analysis

Data were expressed as means ± s.e.m. OriginLab 8.0 software (OriginLab Cooperation, Northampton, MA) were used for statistical analysis (Student's *t*-test and ANOVA). Differences were considered as statistically significant when the calculated *P*-value was less than 0.05.

The authors thank Simon Jungbauer, Melih Kalafat and Christine Mollenhauer for technical assistance; Mohammed Tasab, Charles Streuli and Richard Segar for discussion and proof reading. C.B. acknowledges BBSRC (BB/GG004552/1) and Wellcome Trust (grant 077100) for funding. This publication and the project described herein were also partly supported by the NIH Roadmap for Medical Research (PN2 EY 016586) and by the Excellence Cluster 'CellNetwork' of the

University of Heidelberg. J.P.S holds a Weston Visiting Professorship at the Weizmann Institute, Department of Molecular Cell Biology. The support of the Max Planck Society is highly acknowledged. Deposited in PMC for release after 6 months.

References

Ballestrem, C., Wehrle-Haller, B., Hinz, B. and Imhof, B. A. (2000). Actin-dependent lamellipodia formation and microtubule-dependent tail retraction control-directed cell migration. *Mol. Biol. Cell* **11**, 2999-3012.

Ballestrem, C., Erez, N., Kirchner, J., Kam, Z., Bershadsky, A. and Geiger, B. (2006). Molecular mapping of tyrosine-phosphorylated proteins in focal adhesions using fluorescence resonance energy transfer. *J. Cell Sci.* **119**, 866-875.

Bao, G. and Suresh, S. (2003). Cell and molecular mechanics of biological materials. *Nat. Mater.* **2**, 715-725.

Besser, A. and Schwarz, U. S. (2007). Coupling biochemistry and mechanics in cell adhesion: a model for inhomogeneous stress fiber contraction. *New J. Phys.* **9**, 27.

Chen, C. S., Tan, J. and Tien, J. (2004). Mechanotransduction at cell-matrix and cell-cell contacts. *Annu. Rev. Biomed. Eng.* **6**, 275-302.

Enomoto, T. (1996). Microtubule disruption induces the formation of actin stress fibers and focal adhesions in cultured cells: possible involvement of the rho signal cascade. *Nat. Cell Biol.* **21**, 317-326.

Etienne-Manneville, S. and Hall, A. (2002). Rho GTPases in cell biology. *Nature* **420**, 629-635.

Feige, J. N., Sage, D., Wahli, W., Desvergne, B. and Gelman, L. (2005). PixFRET, an ImageJ plug-in for FRET calculation that can accommodate variations in spectral bleed-throughs. *Microsc. Res. Tech.* **68**, 51-58.

Geiger, B. and Bershadsky, A. (2002). Exploring the neighborhood: adhesion-coupled cell mechanosensors. *Cell* **110**, 139-142.

Geiger, B., Bershadsky, A., Pankov, R. and Yamada, K. M. (2001). Transmembrane crosstalk between the extracellular matrix-cytoskeleton crosstalk. *Nat. Rev. Mol. Cell Biol.* **2**, 793-805.

Geiger, B., Spatz, J. P. and Bershadsky, A. D. (2009). Environmental sensing through focal adhesions. *Nat. Rev. Mol. Cell Biol.* **10**, 21-33.

Haga, J. H., Li, Y. S. and Chien, S. (2007). Molecular basis of the effects of mechanical stretch on vascular smooth muscle cells. *J. Biomech.* **40**, 947-960.

Humphries, J. D., Wang, P., Streuli, C., Geiger, B., Humphries, M. J. and Ballestrem, C. (2007). Vinculin controls focal adhesion formation by direct interactions with talin and actin. *J. Cell Biol.* **179**, 1043-1057.

Ingber, D. E. (2006). Cellular mechanotransduction: putting all the pieces together again. *FASEB J.* **20**, 811-827.

Itoh, R. E., Kurokawa, K., Ohba, Y., Yoshizaki, H., Mochizuki, N. and Matsuda, M. (2002). Activation of rac and cdc42 video imaged by fluorescent resonance energy transfer-based single-molecule probes in the membrane of living cells. *Mol. Cell. Biol.* **22**, 6582-6591.

Iwanicki, M. P., Vomastek, T., Tilghman, R. W., Martin, K. H., Banerjee, J., Wedegaertner, P. B. and Parsons, J. T. (2008). FAK, PDZ-RhoGEF and ROCKII cooperate to regulate adhesion movement and trailing-edge retraction in fibroblasts. *J. Cell Sci.* **121**, 895-905.

Janmey, P. A. and McCulloch, C. A. (2007). Cell mechanics: integrating cell responses to mechanical stimuli. *Annu. Rev. Biomed. Eng.* **9**, 1-34.

Jungbauer, S., Gao, H., Spatz, J. P. and Kemkemer, R. (2008). Two characteristic regimes in frequency-dependent dynamic reorientation of fibroblasts on cyclically stretched substrates. *Biophys. J.* **95**, 3470-3478.

Katsumi, A., Milanini, J., Kiosses, W. B., del Pozo, M. A., Kaunas, R., Chien, S., Hahn, K. M. and Schwartz, M. A. (2002). Effects of cell tension on the small GTPase Rac. *J. Cell Biol.* **158**, 153-164.

Katsumi, A., Naoe, T., Matsushita, T., Kaibuchi, K. and Schwartz, M. A. (2005). Integrin activation and matrix binding mediate cellular responses to mechanical stretch. *J. Biol. Chem.* **280**, 16546-16549.

Kaunas, R., Nguyen, P., Usami, S. and Chien, S. (2005). Cooperative effects of Rho and mechanical stretch on stress fiber organization. *Proc. Natl. Acad. Sci. USA* **102**, 15895-15900.

Kaverina, I., Krylyshkina, O. and Small, J. V. (1999). Microtubule targeting of substrate contacts promotes their relaxation and dissociation. *J. Cell Biol.* **146**, 1033-1044.

Kaverina, I., Krylyshkina, O., Gimona, M., Beningo, K., Wang, Y. L. and Small, J. V. (2000). Enforced polarisation and locomotion of fibroblasts lacking microtubules. *Curr. Biol.* **10**, 739-742.

Kaverina, I., Krylyshkina, O., Beningo, K., Anderson, K., Wang, Y. L. and Small, J. V. (2002). Tensile stress stimulates microtubule outgrowth in living cells. *J. Cell Sci.* **115**, 2283-2291.

Kemkemer, R., Kling, D., Kaufmann, D. and Gruler, H. (2000). Elastic properties of nematoid arrangements formed by amoeboid cells. *Eur. Phys. J. E Soft Matter* **1**, 215-225.

Kodama, A., Karakesisoglou, I., Wong, E., Vaezi, A. and Fuchs, E. (2003). ACF7: an essential integrator of microtubule dynamics. *Cell* **115**, 343-354.

Krendel, M., Zenke, F. T. and Bokoch, G. M. (2002). Nucleotide exchange factor GEF-H1 mediates cross-talk between microtubules and the actin cytoskeleton. *Nat. Cell Biol.* **4**, 294-301.

Krylyshkina, O., Anderson, K. I., Kaverina, I., Upmann, I., Manstein, D. J., Small, J. V. and Toomre, D. K. (2003). Nanometer targeting of microtubules to focal adhesions. *J. Cell Biol.* **161**, 853-869.

Lim, Y., Lim, S. T., Tomar, A., Gardel, M., Bernard-Trifilo, J. A., Chen, X. L., Uryu, S. A., Canete-Soler, R., Zhai, J., Lin, H. et al. (2008). PyK2 and FAK connections to p190Rho guanine nucleotide exchange factor regulate RhoA activity, focal adhesion formation, and cell motility. *J. Cell Biol.* **180**, 187-203.

Liu, B. P., Chrzanowska-Wodnicka, M. and Burridge, K. (1998). Microtubule depolymerization induces stress fibers, focal adhesions, and DNA synthesis via the GTP-binding protein Rho. *Cell Adhes. Commun.* **5**, 249-255.

Liu, W. F., Nelson, C. M., Tan, J. L. and Chen, C. S. (2007). Cadherins, RhoA, and Rac1 are differentially required for stretch-mediated proliferation in endothelial versus smooth muscle cells. *Circ. Res.* **101**, e44-e52.

Putnam, A. J., Cunningham, J. J., Dennis, R. G., Linderman, J. J. and Mooney, D. J. (1998). Microtubule assembly is regulated by externally applied strain in cultured smooth muscle cells. *J. Cell Sci.* **111**, 3379-3387.

Ren, X. D., Kiosses, W. B. and Schwartz, M. A. (1999). Regulation of the small GTP-binding protein Rho by cell adhesion and the cytoskeleton. *EMBO J.* **18**, 578-585.

Schmoranzer, J., Kreitzer, G. and Simon, S. M. (2003). Migrating fibroblasts perform polarized, microtubule-dependent exocytosis towards the leading edge. *J. Cell Sci.* **116**, 4513-4519.

Small, J. V., Geiger, B., Kaverina, I. and Bershadsky, A. (2002). How do microtubules guide migrating cells? *Nat. Rev. Mol. Cell Biol.* **3**, 957-964.

Smith, P. G., Roy, C., Zhang, Y. N. and Chauduri, S. (2003). Mechanical stress increases RhoA activation in airway smooth muscle cells. *Am. J. Respir. Cell Mol. Biol.* **28**, 436-442.

Stamenovic, D., Mijailovich, S. M., Tolic-Norrelykke, I. M., Chen, J. and Wang, N. (2002). Cell prestress. II. Contribution of microtubules. *Am. J. Physiol. Cell Physiol.* **282**, C617-C624.

Suter, D. M., Errante, L. D., Belotserkovsky, V. and Forscher, P. (1998). The Ig superfamily cell adhesion molecule, apCAM, mediates growth cone steering by substrate-cytoskeletal coupling. *J. Cell Biol.* **141**, 227-240.

Tomar, A. and Schlaepfer, D. D. (2009). Focal adhesion kinase: switching between GAPs and GEFs in the regulation of cell motility. *Curr. Opin. Cell Biol*. [Epub ahead of print] doi:10.1016/j.ceb.2009.05.006.

Wang, J. H., Thampatty, B. P., Lin, J. S. and Im, H. J. (2007). Mechanoregulation of gene expression in fibroblasts. *Gene* **391**, 1-15.

Waterman-Storer, C. M., Worthylake, R. A., Liu, B. P., Burridge, K. and Salmon, E. D. (1999). Microtubule growth activates Rac1 to promote lamellipodial protrusion in fibroblasts. *Nat. Cell Biol.* **1**, 45-50.

Wehrle-Haller, B. and Imhof, B. A. (2003). Actin, microtubules and focal adhesion dynamics during cell migration. *Int. J. Biochem. Cell Biol.* **35**, 39-50.

Yamane, M., Matsuda, T., Ito, T., Fujio, Y., Takahashi, K. and Azuma, J. (2007). Rac1 activity is required for cardiac myocyte alignment in response to mechanical stress. *Biochem. Biophys. Res. Commun.* **353**, 1023-1027.

Yoshigi, M., Hoffman, L. M., Jensen, C. C., Yost, H. J. and Beckerle, M. C. (2005). Mechanical force mobilizes zyxin from focal adhesions to actin filaments and regulates cytoskeletal reinforcement. *J. Cell Biol.* **171**, 209-215.

Zaidel-Bar, R., Kam, Z. and Geiger, B. (2005). Polarized downregulation of the paxillin-p130CAS-Rac1 pathway induced by shear flow. *J. Cell Sci.* **118**, 3997-4007.

Zhou, F. Q., Waterman-Storer, C. M. and Cohan, C. S. (2002). Focal loss of actin bundles causes microtubule redistribution and growth cone turning. *J. Cell Biol.* **157**, 839-849.